Optimization of flow distribution in Z-type manifold microchannels

Jinjin Xu [1], Qiang Zhou [2], Huafeng Pan [2], Li Lei [1] and Jingzhi Zhang [1,*]

[1] School of Energy and Power Engineering, Shandong University, Jinan, China

[2] Shanghai JHEAT Technology CO., LTD., Shanghai, China

*Corresponding author e-mail: zhangjz@sdu.edu.cn

Abstract. Electronic components are increasingly being centralized and miniaturized, leading to a rise in heat flux. As a result, there is a growing interest in high heat flux heat dissipation technology. Manifold microchannel (MMC) heat sinks have proven to be effective in dissipating heat from the chip. The Z-type manifold heat sink is more favored in practical applications, because its inlet and outlet are located on both sides, saving space. However, the flow distribution in each microchannel of the Z-type manifold heat sink is more uneven than that in other types of manifold heat sinks. In this paper, deionized water is used as the working medium to explore the influence of different structures of Z-type MMC, which has 40 microchannels, on flow distribution of single-phase flow in Z-type MMCs. By changing the structure of the manifold and the spacing of the fins, the researchers achieved uniform distribution of the flow in the 40 microchannels. Moreover, the optimized formula is applied to Z-type manifold heat sink with different size, and the results show that this MMC can also be optimized.

Keywords: Electronics, High Heat Flux Dissipation Technology, Manifold Microchannel (MMC).

1. Introduction

The advancement of electronic components towards centralization and miniaturization has led to a notable escalation in heat flux, posing a critical thermal management challenge. Consequently, there is a growing focus on high heat flux heat dissipation technologies. Of these solutions, MMC heat sinks stand out for their commendable heat dissipation capabilities designed for chips. In particular, the Z-type manifold heat sink has gained prominence in practical applications due to its structural design with inlet and outlet at both ends, optimizing space utilization. Although the Z-type manifold heat sink has its advantages, a drawback it faces is uneven flow distribution within each microchannel. This presents a key area that requires refinement to enhance performance in real-world scenarios.

Many scholars have conducted research to improve the comprehensive performance of MMC. Raphael Mandel et al. [1] developed a two-phase one-dimensional model for pressure drop and flow distribution in a manifold microchannel system. They found that in single-phase flow, the Z-type manifold provided superior flow distribution to the C-type manifold at low mass flux. The greatest influence on the flow distribution in the Z-type and C-type manifolds is at the manifold outlet. They presented a modeling approach called ‘‘2.5-D”, which could be used to compute heat transfer performance of single-phase flow within less time [2]. Chaowei Chen et al. [3] investigated the flow and heat transfer characteristics of MMCS with different manifold structures by numerical simulation, controlling the manifold converging rate to uniform the distribution of fluid in MMC. Ihsan Ali Ghani et al. [4] constructed a sinusoidal cavity with rectangular ribbed microchannel radiators and compared flow and heat transfer characteristics in the Reynolds number range of 100 to 800. They varied the fin width and length to optimize the overall performance of the radiator. Yuhao Lin et al. [5] considered six types of MMC, namely HU-type, ZU-type, H-type, C-type, Z-type, and U-type, as shown in Figure 1. In the single-phase condition, the thermal performance of Z-type MMC is close to that of H-type. The temperature difference is smaller, but the wall temperature is slightly higher. They recommend useing Z-type MMC in single-phase flow because of its simple structure. In their study, E. Omidbakhsh Amiri et al. [6] use Carboxymethyl cellulose as working fluid, studying the eff used Carboxymethyl cellulose as the working fluid and investigated the effects of different flow

directions. The results show that the flow distribution of the rectangular structure is more uniform than that of other structures.

In this study, we used deionized water to investigate the flow distribution of a single-phase fluid in Z-type MMC within 40 microchannels. By changing the shape of the manifold and the spacing of the fins, the influence of the MMC structure on the flow distribution is explored, and then the optimization scheme is obtained.

2. Numerical Model

In the case of single-phase flow, where there is no evaporation and condensation process of the working fluid, it is considered a heat transfer problem in stable laminar flow. The flow and heat transfer problems of the manifold microchannel heat sink were solved using the computational fluid dynamics software ANSYS-Fluent 2022 R1. The inlet boundary condition is defined as a velocity inlet, while the outlet boundary condition is specified as a pressure outlet. Within the computational domain, the bottom surface serves as the heating surface, with a constant heat flux boundary condition applied. The remaining four faces implement symmetric boundary conditions. The calculation domain is applicable to hexahedral meshes with dimensions of 4.05mm ×0.4mm × 0.45mm.

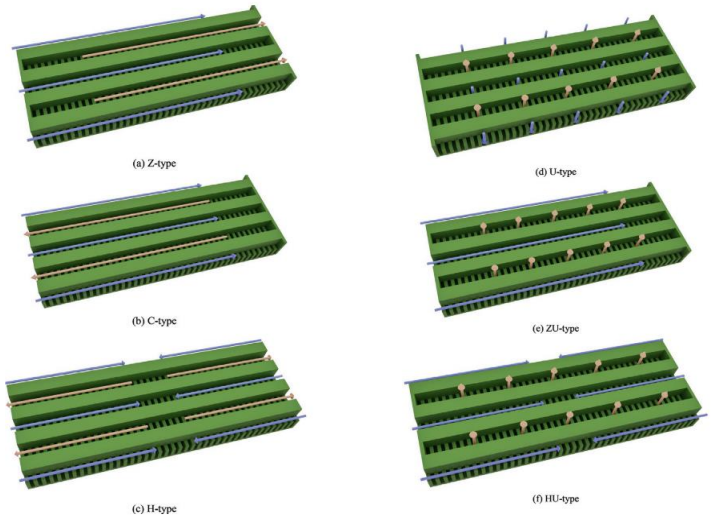

Figure 1. Six types of MMC [5].

Figure 2 shows 5 kinds of MMC partial models, and the specific dimensions and initial conditions are shown in Table 1. Figure 2 (a) shows the original model. deionized water is used as the fluid and the solid material is silicon. Properties of deionized water are k=0.651 W m^{-1} K^{-1}, c_p=4185 J/kg, μ=0.000466 kg m^{-1} s^{-1}, and ρ=983.2 kg/m^3. Silicon has properties k=150 W m^{-1} K^{-1}, c_p=700 J/kg, and ρ=2300 kg/m^3.

3. Establishment of Local Model

The simulation result of the original model case0 is helpful in understanding the flow distribution of 40 branch channels. Accordingly, changes are made to the manifold shape and fins spacing to improve flow uniformity.

3.1 The simulation result of case0

Figure 3 displays the velocity distribution cloud diagram of 40 microchannel sections in case0. It is evident that the flow rates at the heat sink inlet and outlet are higher. The width of each microchannel is consistent, resulting in higher flow rates at both the inlet and outlet. The flow data

and position of each channel are then analyzed and processed. The horizontal coordinate is using this equation:

$$X=i\times L/I \tag{1}$$

where i, L and I indicate the i-th channel from the entrance to the exit, the base length and the total number of channels, respectively. The vertical coordinate is determined by:

$$Y= H\times Q_i/Q_{max} \tag{2}$$

where Q_i, Q_{max} and H represent the flow of the i-th channel, the maximum flow and fin height, respectively. The dimensionless correlation between flow and length is shown in Figure 4 (a).

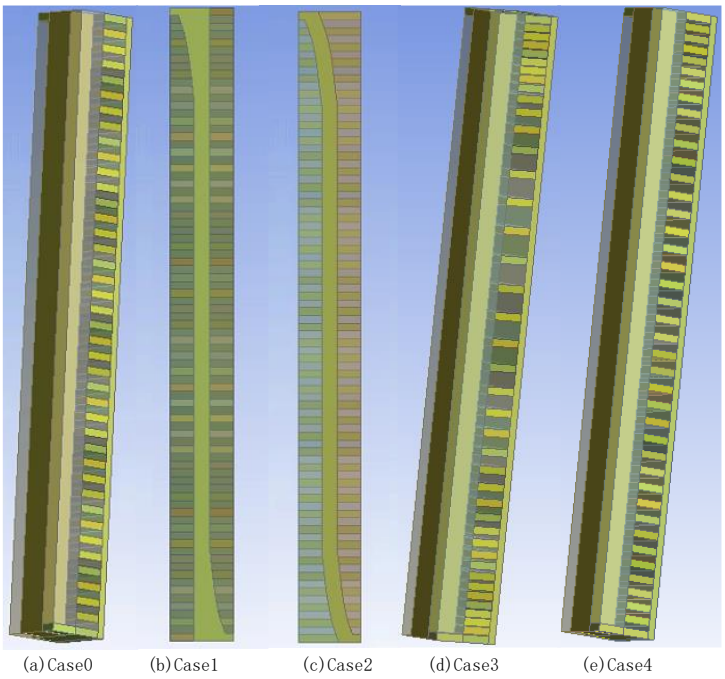

Figure 2. Five kinds of MMC partial models.

Table 1. Specific dimensions of MMCs.

Parameter	Case 0	Case 1	Case 2	Case 3	Case 4
Heat flux (W/cm^2)	100	100	100	100	100
Inlet temperature (K)	303.15	303.15	303.15	303.15	303.15
Inlet velocity (m/s)	1.14	0.76	0.456	1.14	1.14
Inlet area (mm^2)	0.02	0.03	0.05	0.02	0.02
Divider width (μm)	200	equations	equations	200	200
Divider height (μm)	200	200	200	200	200
Fin width (μm)	50	50	50	50	50
Fin height (μm)	200	200	200	200	200
Base height (μm)	50	50	50	50	50

As can be seen from Figure 4 (a), the flow rate of 6 microchannels at the exit is larger. In contrast, the flow rate in the remaining microchannels is more uniform. Therefore, the fitting function about X and Y is fitted in two parts:

$$Y=1.356-0.0015X+0.00000035X^2,\ 0<X<3500 \tag{3}$$

$$Y=-30960.48+25.3X-0.0069X^2+0.00000063X^3,\ X>3500 \tag{4}$$

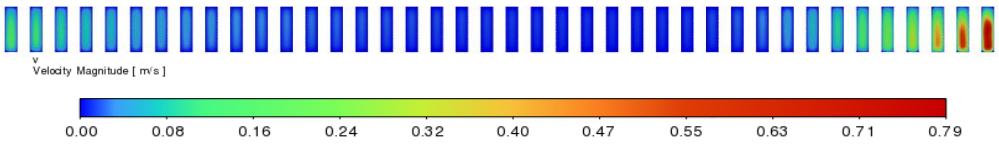

Figure 3. Velocity distribution cloud diagram.

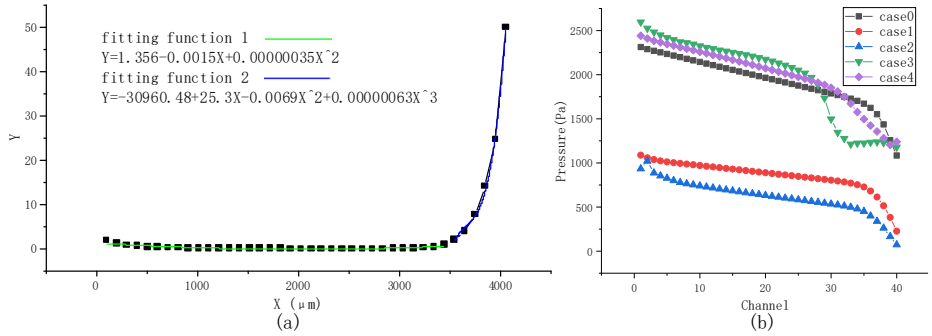

Figure 4. (a) Dimensionless correlation between flow and length; (b) Pressure in each microchannel of the five MMCs.

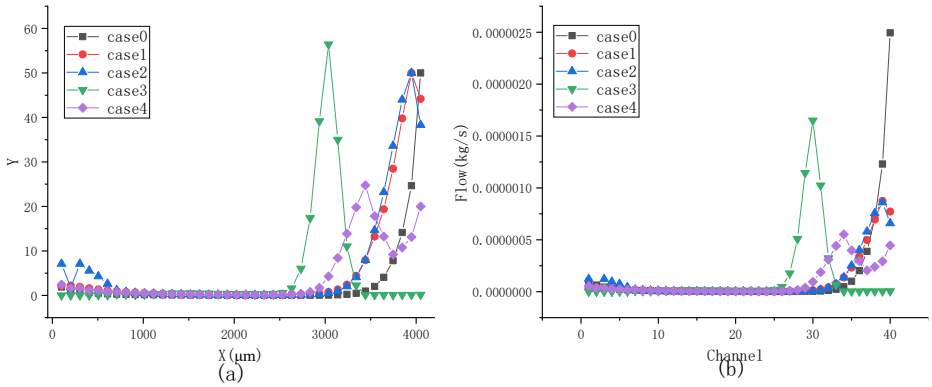

Figure 5. Flow distribution in each microchannel of the five MMCs.

3.2 Manifold Structure Changes

We use the above equation to change the structure of the manifolds. In case1, as shown in Figure 2 (b), from the inlet to 3500μm, the manifold shape adopts the formula (3) on the inlet side, while the rest of the manifold shape adopts the formula (4). The shape of the outlet side and the shape of the inlet side are centrosymmetric. Case 2 increases the inlet area based on Case 1, as shown in Figure 2 (c), and the shape of the manifold above the first six channels is centrosymmetric with that above the last six channels. Divider width is maintained at 100 μm.

3.3 Fins spacing changes

To determine the fins distribution of case 3 and case 4, we define a function according to the flow of each channel. The formula to determine the i-th channel's width, wi, is as follows:

$$w_i = W_c \times b / \Sigma b \tag{5}$$

where W_c represents the sum of all microchannel widths. Additionally, the dimensionless number b, which we define, can be expressed by the following formulas:

$$b = 1/(Q_i/\Sigma Q_i), \text{ in case3} \tag{6}$$

$$b = -\log(Q_i/\Sigma Q_i), \text{ in case4} \tag{7}$$

Case3 is shown in Figure 2 (d), and case4 is shown in Figure 2 (e).

4. Results and Discussion

In this paper, deionized water is used as the working fluid to investigate the flow distribution of single-phase flow in five kinds of manifold microchannels. The inlet temperature of the fluid is 303.15 K and the inlet flow rate is 22.8 mm^3/s. The heat flux of the heat source surface is 100 W/cm^2.

4.1 Pressure analysis

Figure 4 (b) shows the pressure in each microchannel of the five MMCs. It can be seen that the pressure of each channel in case2 is the least, followed by case1. This is because compared with case1, case2 has a larger fluid inlet and outlet area. The manifold widths of case1 and case2 are smaller, and there are more fluid areas in the MMCs, resulting in smoother flow. That's why the pressure in these two cases is lower than in the other three.

4.2 Flow distribution analysis

Figure 5 shows the flow distribution in each microchannel of five MMCs, where (a) represents the dimensionless correlation between flow and the length of the microchannels in the five MMCs, and (b) illustrates the flow distribution in the microchannels of the five MMCs. It was observed that the most uniform distribution of traffic is in case4. Microchannels with uneven flow are concentrated at the exit location, as in case4. Although the inlet pressure is significantly reduced in case1 and case2, the flow rate of the microchannels at the exit is still much higher than that of the other microchannels. Case3 and case4 reduce the area of the microchannels with high flow in the original MMC, so the flow at the exit of these two cases is reduced. However, the microchannel area in the middle area of case3 is too large, resulting in high flow in some channels, and the overall flow distribution of the MMC is still uneven. In comparison to the other three schemes, the optimization impact of case4 is substantial.

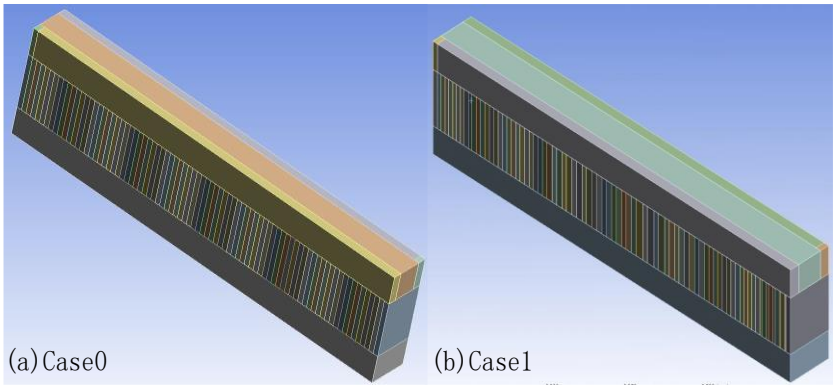

Figure 6. Before and after optimization models.

4.3 Other sizes MMCs

In summary, case 4 exhibits the most consistent flow distribution results. We apply the optimization formula to MMC of different sizes to assess the applicability of the optimization scheme. The base height, base width, fin height, manifold height and manifold width of the newly constructed model are 100 microns, 172 microns, 200 microns, 100 microns and 100 microns, respectively. The fin width and adjacent spacing of the original model are 20 microns, as shown in Figure 6 (a). According to the optimization formula in case4 above, the fin spacing of the original model was adjusted to obtain the model shown in Figure 6 (b).

The simulation results are shown in Figure 7. Figure 7 (a) shows the comparison of pressure in each microchannel of the before and after optimization. Figure 7 (b) illustrates the comparison of flow distribution in MMCs before and after optimization. It is evident that following optimization, there is an increase in pressure in the majority of microchannels. Additionally, the uniformity of flow distribution in the microchannels shows significant improvement. The maximum microchannel flow

is reduced by more than double. It can be concluded that the formula in case 4 can effectively optimize the flow distribution in Z-type MMCs of various sizes.

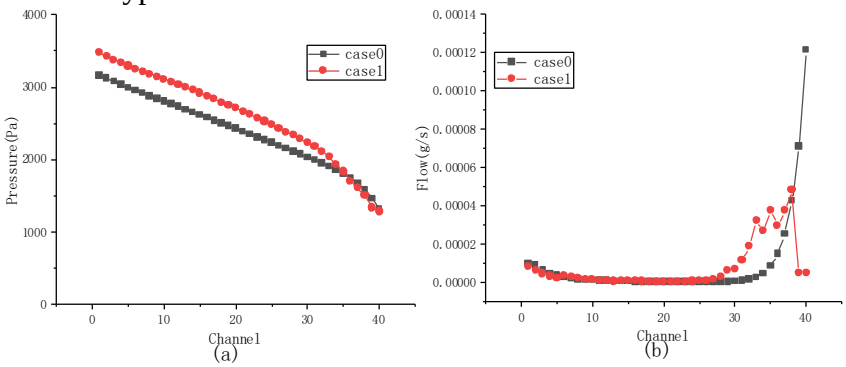

Figure 7. Comparison of pressure and flow distribution before and after optimization.

5. Conclusion

By changing the manifold structure and fin spacing of the original Z-type MMC, we obtained four optimization cases. The numerical simulation results of single-phase flow for five Z-type MMCs with different structures were compared. We calculate the pressure and flow rate of each microchannel, and analyze the influence of different structures on the flow distribution. The optimal scheme is applied to MMC of different sizes, and the following conclusions are drawn:

(1) Optimizing the manifold structure can effectively decrease the microchannel pressure, but it may not be beneficial for enhancing the uniformity of flow distribution.

(2) Adjusting the fin spacing can effectively average the flow distribution of Z-type MMC, but this adjustment also results in increased pressure.

(3) Case4 has the best uniform flow distribution, and its optimization formula is suitable for different sizes of Z-type MMC.

References

[1] Mandel,R. , Shooshtari,A. ,& Ohadi , M.(2018).Effect of manifold flow configuration on two-phase ultra-high flux cooling.Numerical Heat Transfer, Part A: Applications,74(8),1425-1442.

[2] Mandel,R. , Shooshtari,A. ,& Ohadi , M.(2018).A “2.5-D” modeling approach for single-phase flow and heat transfer in manifold microchannels.International Journal of Heat and Mass Transfer,126(),317-330.

[3] Chen,C. , Wang,X. , Yuan,B. , Du,W. ,& Xin , G.(2022).Investigation of flow and heat transfer performance of the manifold microchannel with different manifold arrangements.Case Studies in Thermal Engineering,34(),102073.

[4] Ghani,I.A. , Kamaruzaman,N. ,& Sidik , N.A.C.(2017).Heat transfer augmentation in a microchannel heat sink with sinusoidal cavities and rectangular ribs.International Journal of Heat and Mass Transfer,108(),1969-1981.

[5] Lin,Y. , Luo,Y. , Li,W. , Cao,Y. , Tao,Z. ,& Shih , T.I.(2021).Single-phase and Two-phase Flow and Heat Transfer in Microchannel Heat Sink with Various Manifold Arrangements.International Journal of Heat and Mass Transfer,171(),121118.

[6] Omidbakhsh amiri,E. ,& Ghasemi ahmad chali M.(2020).Numerical Studies of Flow and Temperature Distribution in a Micro-heat Exchanger.Arabian Journal for Science and Engineering,45(9),7667-7675.